Characterization of Laminar Jet Impingement Cooling in Portable Computer Applications

John R. Guarino
Raytheon Systems Co.
Naval and Maritime Integrated Systems
Portsmouth, RI 02871
John_R_Guarino@RES.Raytheon.com

Vincent P. Manno*
Dept. of Mechanical Engineering
Tufts University
Medford, MA 02155
Vincent.Manno@Tufts.edu
* Corresponding author

Abstract - A thermal characterization study of laminar air jet impingement cooling of electronic components within a geometry representative of the CPU compartment of a typical portable computer is reported. A finite control volume technique was used to solve for the velocity and temperature fields. Convection, conduction and radiation effects were included in the simulations. The range of jet Reynolds numbers considered was 63 to 1500; the applied compartment heat load ranged from 5W-15W. Radiation effects were significant over the range of Reynolds numbers and heat loads considered, while the effect of natural convection was only noticeable for configurations when the ratio Gr/Re^2 exceeded 5. The predicted importance of Re rather than jet size was confirmed with test data. Proof of concept was demonstrated with a numerical model representative of a full laptop computer. Both simulations and lab tests showed that low flow rate JI cooling schemes can provide cooling comparable to a high volume flow rate configuration, while using only a fraction of the air flow. Further, under the conservative assumption of steady state, fully powered components, a hybrid cooling scheme utilizing a heat pipe and laminar JI was capable of cooling the processor chip within to 11C of the vendor specified maximum temperature for a system with a total power dissipation of over 21 W.

Index Terms – jet impingement, laminar flow, portable computers, heat pipe

Nomenclature

D_h	Jet hydraulic diameter (m)
Gr	Grashof number ($g\beta\Delta TL^3/\nu^2$)
H	Compartment Height (m)
h	Heat transfer coefficient (W/m^2K)
k	Thermal conductivity (W/mK)
L	Characteristic length (m)
Nu	Nusselt number ($q''L/\Delta Tk$)
P	Power dissipation (W)
p	Pressure (Pa)
Pr	Fluid Prandtl number
Q	Heat flow (W)
q”	Heat flux (W/m^2)
Re	Reynolds number (VD_h/ν)
T	Temperature (C)
u	Velocity in the x direction (m/s)
V	Average jet velocity (m/s)
v	Velocity in the y direction (m/s)
w	Velocity in the z direction (m/s)
W	Jet width (m)
α	Thermal diffusivity (m^2/s)
β	Coefficient of volume expansion (1/K)
ν	Kinematic viscosity (m^2/s)
θ	Thermal resistance (C/W)
ε	Emissivity

I. Introduction

The current trend in the electronics industry is one of increased computing performance, combined with the unending demand for portability and increased miniaturization. As power dissipation values increase, and the size of the electronics enclosure decreases, engineers are continuously challenged to find novel thermal management techniques to ensure adequate cooling. Laptop computers pose a significant thermal management problem due to the desire to have the computing capabilities of the desktop computer in a portable platform. Due to space limitations, laptop computers have higher power densities than desktop computers that use the same processor chips. Additionally, the high volume flow rate forced convection cooling schemes that are used in desktop computers are not applicable to laptops due to space and battery power constraints.

The literature already contains serious consideration of advanced cooling techniques for portable computers. In designing a thermal management scheme for an ultra-slim laptop (approx. 12 mm thick), Kobayashi *et al.* [1] studied the possibility of using a high thermal conductivity Magnesium plate to spread processor heat from the motherboard to the laptop walls. Rujano *et al.* [2] proposed several thermal management plans using heat pipes to transport processor heat to external heat sinks. Campbell *et al.* [3] experimentally studied the use of pulsating, synthetic micro-jets to provide additional cooling for laptop processor chips. A comprehensive study related to thermal modeling of high performance processor chips in laptop computers was completed by Viswanath *et al.* in [16]. The configuration analyzed by Viswanath *et al.* was cooled by natural convection and considered several enhancement techniques, including heat pipes. The use of heat pipes to cool laptop computers was also considered by Xie *et al.* in [4] and Nguyen *et al.* in [5].

This paper considers the possibility of enhanced cooling of laptop microprocessor chips via laminar air jet impingement (JI), that is, impinging a low velocity stream of air directly on the surface of the microprocessor chip to enhance cooling. JI heat transfer is attractive due the high convective heat transfer rates that can be achieved in the stagnation region of the flow, even with very low mass flow rates. Due to the extremely low flow rates required, laminar JI provides "nearly" passive thermal management, which allows for the use of smaller prime movers, causing minimal drain on the system battery.

This work focuses on identifying the design parameters that affect JI thermal management. The following fundamental questions arise regarding the use of JI in portable computing applications:

- Does JI heat transfer enhance cooling, relative to natural convection alone?
- What effect does the shallow enclosure geometry have on the various heat transfer modes?
- Under what conditions does buoyancy affect the overall thermal solution?
- What is the contribution of each heat transfer mode and under what conditions are they important?
- What is the maximum processor power dissipation that can be achieved in a typical laptop computer using laminar JI?

Three-dimensional numerical models of an Intel® Mobile Pentium® III Processor mounted on a motherboard, in a compartment representative of a typical portable computer were generated. The numerical models included conduction, convection and radiation heat transfer effects. The configuration was analyzed by completing parametric studies to investigate the effect of the following: jet velocity, jet size (cross section), spacing between the jet and target surface, processor power dissipation, and compartment venting conditions. Computed results were compared to test data to verify the reasonableness of the predictions. The results of the parametric studies were used to analyze a full laptop computer model in order to demonstrate proof of concept thermal management designs that included JI-only and hybrid/JI-heat pipe strategies.

II. BASICS OF LAMINAR JET IMPINGEMENT AND MODEL VERIFICATION

Impinging jets are used in applications that require localized and efficient transfer of heat, and high heat transfer rates such as annealing of metals and plastics, cooling of turbine blades, drying of textiles, and the cooling of high power dissipation/high heat flux electronic components. While there exist many possible configurations for impinging jets, an understanding of the basic transport phenomena can be obtained by considering the simplified configuration shown in ***Figure 1***.

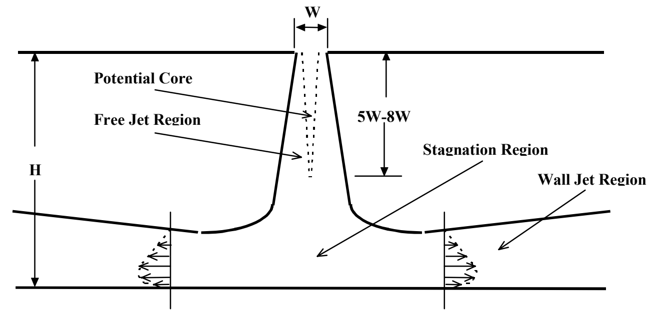

Figure 1 *- Schematic of Impinging Jet*

Typically, the flow pattern of impinging jets can be sub-divided into three regions: free jet region, stagnation flow region and the wall jet region. The free jet region may be further sub-divided into the following regions: potential core, developing jet flow and developed jet flow region. The length of the potential core is generally 5-8 times the jet width [6]. The stagnation region is characterized by an increase in static pressure, resulting from the abrupt axial deceleration of the jet at the impingement surface. The stagnation point is characterized by a maximum in static pressure and zero flow velocity. After impingement, the flow deflects in the transverse direction and begins to accelerate due to the favorable pressure gradient, thus beginning the transition to wall jet flow.

The bulk of the existing JI literature addresses turbulent flow configurations. However, there are some numerical and a few experimental studies dedicated to laminar impinging jets. A numerical study was performed by Wheeler and Neti [7] that considered heat transfer and fluid flow characteristics of a confined laminar air jet impinging on a heated surface. Local Nusselt number values along the target surface were found to form a bell shaped distribution, with a maximum at the stagnation point. The stagnation region Nusselt numbers were found to depend on the square root of the jet Reynolds number.

Experimental JI studies were completed by Ichimiya *et al.* in [8] and Lin *et al.* in [9]. Both studies were of confined slot jets impinging on heated surfaces. In both cases stagnation region Nusselt numbers were found to depend on the square root of the jet Reynolds number. A significant portion of the Lin study was dedicated to determining the jet Reynolds number that demarcated the end of the laminar regime. According to the results of Lin, low level turbulence was found to occur at the jet mouth when the Reynolds number exceeded 1500.

The numerical simulations reported in this paper were completed with FLOTHERM™ 2.2, a commercially available finite control volume code. The configurations of [7], [8] and [9] were modeled to gain insight into any subtleties associated with modeling laminar jets, and to provide confidence in the subsequent numerical calculations of this work. In all cases there was excellent agreement between the numerical predictions of this author and the previously published experimental and numerical results.

Figure 2 shows a plot of the Nusselt number along the target surface for the experimental configuration of Ichimiya *et al.* ***Figure 3*** plots the stagnation point Nusselt number versus the square root of the Reynolds number for three verification cases completed. Further, the constant slope of the plots demonstrates the classic dependence of stagnation region heat transfer on the square root of the jet Reynolds number. The agreement of the predictions with literature data indicates that the transport phenomena have been successfully captured with the numerical simulations. The results of the verification studies provide confidence in the subsequent thermal characterization study.

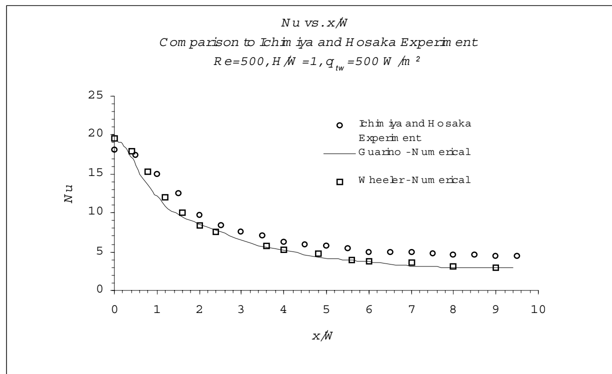

Figure 2 *- Nusselt Number Profile, Comparison to Ichimiya and Hosaka*

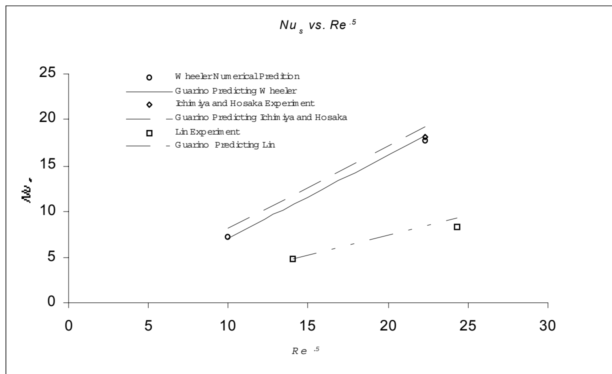

Figure 3 *– Summary of Stagnation Region Nusselt Numbers*

III. SIMPLIFIED PORTABLE CPU COMPARTMENT PARAMETRIC STUDY

Figure 4 shows the model of the simplified compartment used for the parametric study. The compartment size is 127mm x 25.4mm x 102mm and is based on typical motherboard sizes reported in [1], [2], [3], [4], and [5]. The model contains six walls (3 are hidden for clarity in ***Figure 4***), a motherboard, processor chip, jet and an outlet vent. The jet is located directly above the processor chip, and the processor chip is centered in the X-Z plane of the motherboard.

Air enters the compartment at the jet and exits through the outlet vent. The ambient air temperature was specified as 25C. The compartment walls were modeled with a constant wall temperature boundary condition (T_{wall}=35C).

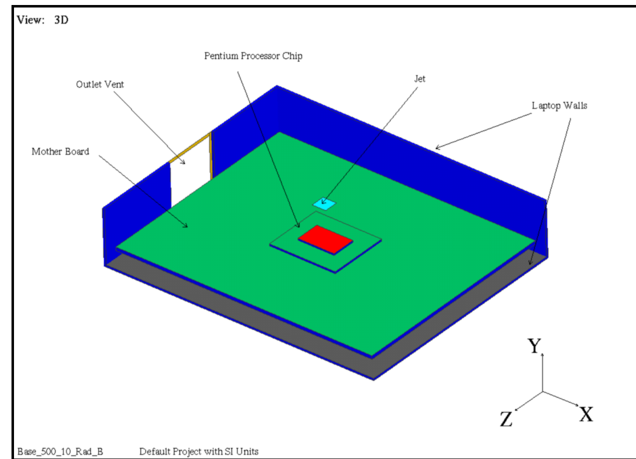

Figure 4 *– FLOTHERM™ Model of Simplified Compartment*

The processor chip represented in the simulations is an Intel® Mobile Pentium® III microprocessor commonly used in portable computing applications. The chip consists of an Organic Land Grid Array substrate (OLGA) and a Silicon die. The OLGA substrate (27mm x 31mm x 1mm) attaches to the board with solder balls. The die (11mm x 17 mm x .9mm) mounts face down on the substrate (i.e. flip chip style) and was modeled as with the properties of pure silicon. The details of the thermal characteristics of the chip were obtained from [12] and from conversations with Intel® technical support engineers. Details of the model of the chip are included in [11].

To reduce the computational overhead, radiative exchange was allowed between the surfaces that contributed significantly to the radiation heat transfer, namely: compartment inside top and bottom walls, top surface of die, top surface of substrate, top and bottom surfaces of motherboard. Details of material properties used in the simulations are listed in ***Table 1***, while a summary of the physical configuration of the compartment is shown in ***Table 2***.

Table 1 *– Material Properties Summary*

Component	Material	Thermal Conductivity, k {W/mK}	Emissivity, ε
Die	Pure Silicon	k(T) = 117 - .42(T - 100)	0.65
OLGA Substrate	Composite	23.0*	0.90
Die attach (solder/epoxy)	Solder/epoxy	2.9*	-
Chip attach	Solder (63 % Sb, 37 % Pb)	55.0	-
Motherboard	Composite	20 (in-plane), .35 (through-plane)	0.90
Compartment walls	Infrared opaque plastic	-	0.95

* Indicates effective value

Table 2 – Summary of Simplified Compartment

Compartment size:	127mm x 102mm x 25.4mm
Mother board size:	120mm x 95mm x1.6mm
Jet size:	6.35 mm, square
Jet/target spacing: (H/W)	2.5
Jet location:	Centered on chip
Chip location:	Centered on mother board
Number of vents:	1
Vent size:	25.4mm, square
Vent location:	Centered on X-low wall
Number of grid cells (X x Y x Z):	75 x 59 x 75
Chip power:	10 W
Mother board power:	0 W
Radiation:	On
Buoyancy:	On
Jet Inlet Temperature	25 C
Wall Temperature	35 C
Jet Reynolds number:	500, 1000, 1500

A. *Thermal Characteristics of Baseline Simplified Compartment*

Next the thermal characteristics of the baseline compartment are considered. Three jet flow rates were utilized to establish the baseline compartment thermal characteristics: V_{jet}=1.25m/s, 2.5m/s, 3.75m/s which correspond to Re =500, 1000 and 1500, respectively. As expected, the jet Reynolds number significantly affected the thermal performance. The average predicted die temperatures were 125C (Re=500), 113C (Re=1000) and 105C (Re=1500).

Figure 5 is a plot of the motherboard surface temperature versus position (x/W=0 corresponds to the centerline of the jet) for these three cases. The location of maximum temperature at the jet centerline corresponds with the center of the die heat source. ***Figure 6*** shows the respective motherboard temperature contours. The effect of the jet Reynolds number is clear. The average motherboard temperatures predicted were 86C, 78C, and 73C, for Re = 500, 1000 and 1500, respectively.

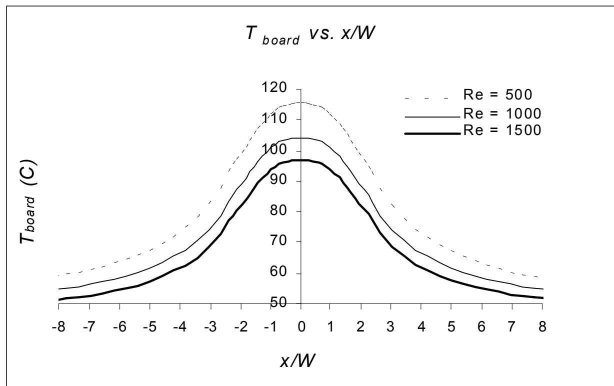

Figure 5 *- Board Temperature vs. Position for Baseline Simplified Compartment (die: -1.3<x/W<1.3,substrate: -2.4<x/W<2.4)*

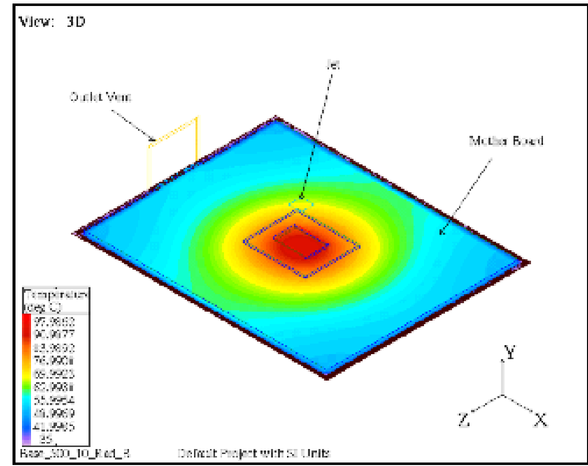

(a)

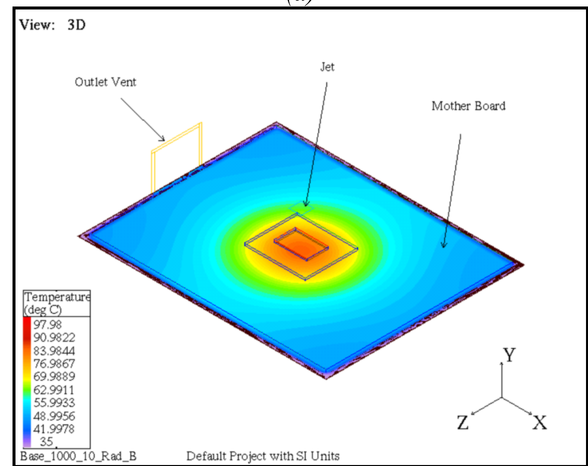

(b)

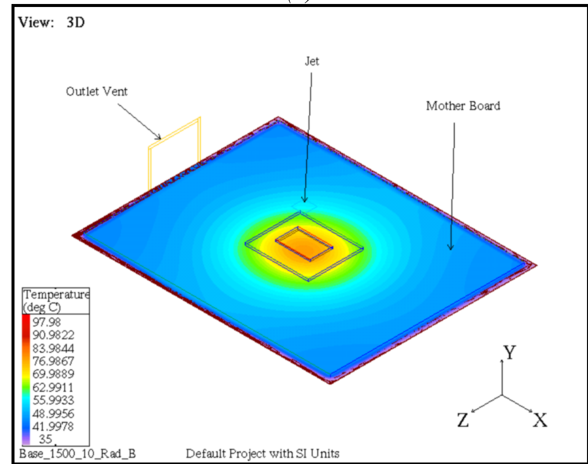

(c)

Figure 6 *- Motherboard Temperature Contours for Simplified Configuration (a) Re = 500, (b) Re = 1000, (c) Re = 1500*

Sensitivity studies were completed to characterize the effects of material property variation, imposed wall temperature and computational grid on the predicted die temperature. The details of the sensitivity studies can be found in [10] and [11]. The effect of variations in the following material properties was studied: chip substrate effective conductivity, die attach effective conductivity, compartment wall emissivity, chip substrate emissivity and motherboard emissivity. The emissivity values were varied

by 10%, while affecting the die temperature rise by about 1%. The thermal conductivity values were varied by 40% while the die temperature rise was affected by less than 4%. It was determined that 5C variations in wall boundary temperature resulted in die temperature variations of approximately 2C.

Regarding the finite volume grid, it was found that the results were most sensitive to the number of vertical cells used between the jet and the top surface of the die, due to the steep thermal and velocity gradients associated with the impinging flow. Grid independent results were obtained when at least 15 grid cells/jet width of vertical spacing were used. A non-uniform, Cartesian grid was used with 47% of the cells concentrated within 1 jet width of the top surface of the die.

B. Synthesis of Parametric Studies

The thermal characterization of the baseline compartment focused on the effect jet/die (H/W) spacing, jet size (cross section) and compartment venting conditions. The separate effects of natural convection and radiation were also considered. Unless otherwise specified, the only heat applied was the chip heat load of 10W. For certain cases the chip heat load was reduced to 5W and some cases included an additional 5W of heat spread evenly over the motherboard to account for heating due to other components on the motherboard.

Table 3 summarizes the limits of laminar JI, as observed with the parametric studies of the baseline compartment. Assuming that the maximum jet Reynolds number that can be used within the laminar regime is Re=1500 (per the experimental finding in [9]), it is clear that the maximum chip power dissipation that can be cooled with a laminar jet is approximately 10W. The addition of the 5W to the motherboard increased the predicted die temperature to approximately 113C.

Table 3 *– JI Results for Simplified Baseline Compartment*

Re	Processor Heat Load (W)	Additional Mother Board Heat Load (W)	Predicted Die Temp. (C)
1500	10	-	105
1500	10	5	113
1500	5	-	68
63	5	-	90

The results of the parametric studies with a processor heat load of 5W are relevant to the application of laminar JI to lower power systems. As is shown in ***Table 3***, a jet with a Reynolds number of only 63 was able to cool the processor die to below 100C. The results indicate that low Re laminar JI (Re<500) by itself may be useful for cooling moderate power dissipation components in portable applications, specifically, components with power dissipations that are just high enough to make natural convection only cooling schemes unreliable.

In considering the compartment physical arrangement, it was found that jet size (cross section) had more effect on the cooling of the die than did jet/die spacing or the venting conditions. Larger jets resulted in cooler bulk air temperatures exiting the compartment (due to the increased mass flow rate for a given Reynolds number), while smaller jets resulted in slightly cooler die temperatures (due to the increase heat transfer coefficient for a given Reynolds number). The effect of jet size was most noticeable at higher Reynolds numbers, where the 6.35mm square jet resulted in a 3C cooler die temperature (105C vs. 108C) than the 11mm x 17mm jet at Re=1500.

There can be decreased heat transfer from the target surface for JI configurations with high jet to target surface spacing (H/W>8). However, with this shallow compartment, even for the cases involving the lowest Reynolds number jets, the jet potential core extended to the target surface. Hence, there were no further gains in thermal performance to be made by moving the jet closer to the target surface.

Venting conditions were found to have little effect on the temperature of the die. Changing vent cross sectional area, relative to the baseline area, was found to have no effect on the temperature of the chip. The results also showed that the die temperature was insensitive to the location of and number of outlet vents. In practice, it is probably better to vent laptop JI configurations from the sides of the compartment, rather than from the top. Vents located on the top surface of a laptop computer are more likely to become inadvertently obstructed by the user, and there is also an increased risk of spilling liquids or foreign matter into the compartment.

Radiative heat transfer was found to be significant over entire range of jet Reynolds numbers (500-1500) and the compartment heat loads (5W-15W) analyzed. As expected, radiation effects were most significant for low Reynolds number, high power applications. For the baseline compartment, the contribution of radiation to the overall heat transfer from the compartment was 25% for Re=1500 and 42% for Re=500. For Re=250, with a processor chip heat load of 10W, neglecting radiation increased the predicted die temperature from 125C to 149C. Even with a chip heat load of 5W and Re=1500, radiation effects were still relevant, as neglecting radiation increased the die temperature from 68C to 72C.

The effect of natural convection on the overall thermal performance was not as dramatic as the effect of radiation. The importance of buoyancy to the overall heat transfer was found to depend on the ratio Gr/Re^2. High values of Gr/Re^2 indicate that buoyancy effects dominate the flow, while low values of Gr/Re^2 indicate that buoyancy effects are negligible, compared to the forced component of the flow. Gr/Re^2 values of order 1 indicate the presence of a mixed convection flow regime.

Over the range of Re=63-1500, heat transfer from the die was essentially unaffected by buoyancy, for P_{chip}=5W and

P_{chip}=10W. The results are expected given the low value of the ratio Gr/Re^2 (from .05 to .2) in the die region, indicating that due to the flow of the jet, forced convection effects are dominant. Note that the characteristic lengths used in evaluating Gr for the die and board, were the die half-width and the board half-width, respectively. In contrast, the characteristic length in computing Re is the jet width. The decrease in die temperature that occurred for cases that included natural convection was due to increased heat transfer from the board which in turn lowered the temperature of the chip die.

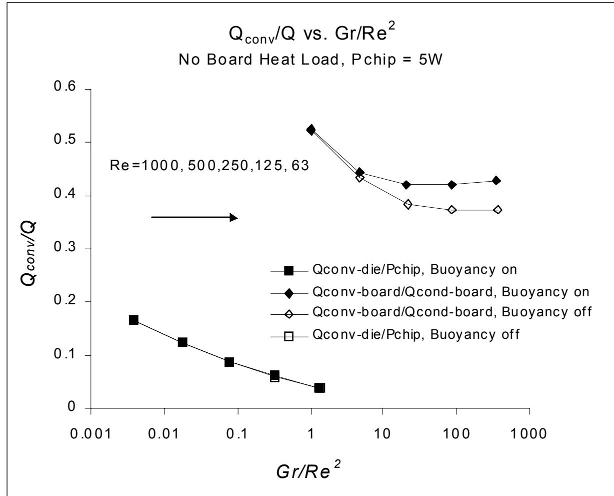

***Figure** 7 – The Effect of Buoyancy on Heat Transfer from the Die and Motherboard*

For the case with P_{chip}=5W, with no additional heat applied to the motherboard, buoyancy was found to increase the heat transfer from the motherboard when the jet Reynolds number was 500 or below. Increasing the chip power to 10W and adding an additional 5W of heat to the motherboard made buoyancy effects on the heat transfer from the motherboard noticeable when the jet Reynolds number was 1000 or less. For the two cases mentioned, the effect of buoyancy on the heat transfer from the motherboard became noticeable at different jet Reynolds numbers; however, the value of Gr/Re^2 when buoyancy effects became noticeable was approximately 5 for both cases. (See ***Figure** 7*) Including the effect of buoyancy was found to decrease the predicted die temperature by about 2C for the case of Re=125 and P_{chip}=5W and Gr/Re^2 =375.[1]

C. Experimental Verification of Predictions

An experiment was conducted to test the validity of the CPU compartment parametric study results. A Sony Vaio™ computer containing a 333 MHz Intel Pentium II™ was modified by removing the integrated CPU fan/heat sink assembly and positioning round plastic tubing above the CPU through which low flow air was directed. The tubing was of sufficient length from the air source that a fully developed velocity profile would be obtained, which is different from the uniform profile assumed in the numerical study. The CPU compartment was similar to the simulation model except the CPU was somewhat offset from the center and there was a large bus controller package mounted in the vicinity of the CPU.

Three jet diameters (4.3mm, 6.4mm, and 9.5mm) were employed at Re of 500, 1000, and 1500. This testing range yielded the volumetric flowrates summarized in Table 4.

***Table 4** - Volumetric Flowrates (10^{-4} m^3/s)*

		Jet Diameter		
		4.3mm	*6.4mm*	*9.5mm*
Re	*500*	*0.19*	*0.28*	*0.35*
	1000	*0.38*	*0.56*	*0.84*
	1500	*0.76*	*0.84*	*1.25*

These jet flowrates can be compared to the integral fan/heat sink module flow of 6.30x10^{-4} m^3/s. The modified laptop was instrumented with Type T thermocouples. Steady state CPU surface temperatures are reported in Table 5.

***Table 5** - CPU Temperature (C above ambient).*

		Jet Diameter		
		4.3mm	*6.4mm*	*9.5mm*
Re	*500*	*88±4*	*83±1*	*82±2*
	1000	*69±1*	*72±2*	*69±2*
	1500	*59±3*	*62±1*	*60±1*

The data in Table 5 confirm the prediction that Re, not jet size, is the dominant thermal control parameter. Note that the measured CPU temperatures for all jet diameters at the same Re agree to within experimental uncertainty. The CPU temperature change with Re is in good agreement with the predictions listed in section III.A above.

The effectiveness of laminar JI cooling can be observed by noting that the original high flow rate fan/heat sink assembly yielded a CPU surface temperature of approximately 52C above ambient. Hence a 4.3mm, Re=1500 jet produced cooling similar to the original design with approximately one-eighth the volumetric flowrate. This would translate to a fan power consumption reduction of well over 50% and a commensurate noise reduction.

IV. APPLICATION TO PROTOTYPIC SYSTEM

To demonstrate proof of concept, the results of the parametric studies and the verification tests were used to simulate JI cooling in a full laptop computer model. The baseline compartment was enlarged to the size of a typical laptop computer and the various subassemblies typically found in portable computers were added to the numerical model. The basic characteristics of the chip model and board model used in the simplified compartment were unchanged in the full model.

[1] For details of the radiation and buoyancy analyses as well as information regarding a peculiar mixed convection regime that was observed, the reader is referred to [10] and [11].

A. Description of Full Sized JI Configuration

Figure 8 shows the numerical model of the full sized compartment (the compartment walls are hidden for clarity). The jet impinges on the processor chip in the same fashion as the simplified model. Air enters the computer at the jet at 25C and exits through the outlet vent to the ambient. All of the solids within the compartment, including the compartment walls, were treated as thermally conductive solids with the material properties specified in ***Table 6***. Rather than modeling the details of the various assemblies, the drives, battery, PCMCIA cards, power supply board and keyboard were modeled with effective thermal conductivity values.

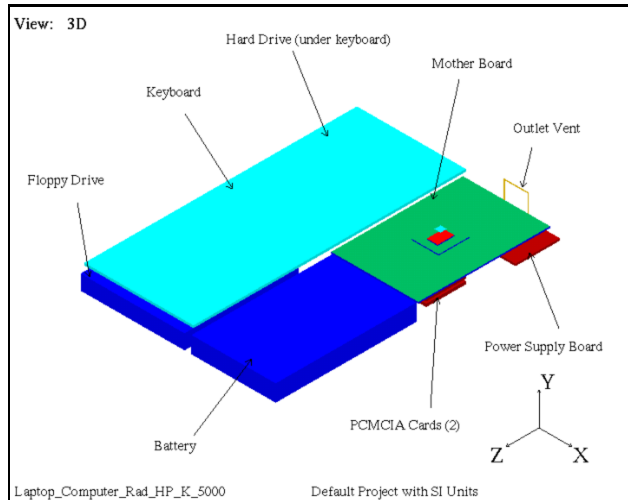

Figure 8 *– FLOTHERM™ Model of Full Sized Laptop*

Table 6 *– Summary of Full Sized Laptop Configuration*

	Size (mm)	k (W/mK)	k Source	ε	ε Source	P(W)
Overall Size	210 x 25.4 x 295	-	-	-	-	-
Jet	6.4 x 6.4	-	-	-	-	-
Outlet Vent	25.4 x 25.4	-	-	-	-	-
Hard Disk Drive	90 x 15 x 110	25	[13]	-	-	2
Floppy Disk Drive	105 x 15 x 115	25	[13]	-	-	0.3
Battery	85 x 17 x 142	25	[13]	-	-	1.5
Power Supply Board	95 x 2 x 45	25	[13]	0.9	[13]	1.5
PCMCIA Cards (2)	70 x 3 x 40	25	[13]	0.9	[13]	.5 (each)
Keyboard	110 x 2.5 x 275	25	[13]	0.5	[15]	-
Motherboard	88 x 1.6 x 133	20 in plane, .35 through plane	[13]	0.9	[13]	5
Processor Chip	27 x 1.9 x 31	-	-	-	-	10
Compartment Walls	-	0.4	[15]	0.95	[14]	-
					Total:	21.3

For the baseline configuration, the temperature of the compartment walls specified at 35C. For the full model, the compartment walls were treated as thermally conductive and the wall temperature was predicted, rather than specified. Heat was allowed to exit all of the compartment walls to the ambient via natural convection. Specifying the heat transfer coefficient for the outside surfaces approximated the natural convection heat transfer to the ambient. Correlations from [15] were used to approximate the heat transfer coefficients for heated horizontal and vertical walls cooled by natural convection.

The expression used for the heat transfer coefficient from the vertical walls is listed as follows:

$$h = 1.07*[(T_{wall}-T_o)/y]^{.25} \qquad (1)$$

where: T_o = 25C, and y = vertical position along wall.

Equation 1 was integrated along the height of the wall to obtain an average heat transfer coefficient. The resulting average heat transfer coefficient was applied to all external, vertical walls. In a similar manner, the average Nusselt number for the laptop Y-high, horizontal wall was approximated with *Equation 2*.

$$Nu = .54*[\{\beta(T_{wall}-T_o)*g*x^3\}/\nu*\alpha]^{.25} \qquad (2)$$

In application, typical laptop computers have rubber mounting feet on the Y-low compartment wall. The mounting feet contact the surface that the computer sits on, leaving a small gap (about 2-3mm) between the compartment Y-low wall and the surface. It was assumed that heat exits the compartment Y-low wall via conduction through the air gap to the mounting surface. The mounting surface was assumed to be isothermal at a temperature elevated 5C above the ambient temperature of 25C. Rather than modeling the air gap and the mounting surface, an effective heat transfer coefficient was specified on the Y-low wall. The effective heat transfer coefficient that was used results in the same thermal resistance between the wall and the mounting surface that would occur as a result of conduction through a 3mm air gap. The grid used in the full model (≈340k cells) followed the guidelines for grid independent results established in **III**.

B. Comparison Between Simplified and Full Models

The average die temperature predicted for the full laptop was approximately 131C, well above the desired die temperature of 100C and 18C above the predicted die temperature for the baseline compartment. The wall boundary condition was considered as one possible explanation for this difference. For the simplified configuration, all compartment wall temperature were specified and held constant (35C), effectively forcing the walls to behave as infinite heat sinks. The average wall temperatures predicted by the full model ranged from 32C to 47C (the Y-high wall was the hottest). Recalling the sensitivity cases that are described **IIIA**, a 5C increase in wall temperature resulted in an increase in die temperature of about 2C for the simplified configuration. Assuming a similar dependence for the full model, if all of the walls were at maximum temperature of 47C, the predicted die temperature should only increase by about 5C. Further, based on the wall temperatures predicted by the full model (42C, 32C, 47C, 42C, 32C, 45C) the assumed wall temperature of 35C appears to have been a reasonable assumption for the simplified compartment. It is clear that the wall temperature boundary condition by itself does not account for the increase in predicted die temperature.

Figure 9 contains side view temperature contours, taken at the centerline of the jet in the stream-wise direction. It is clear that the heat generated by the PCMCIA cards and the

power supply board is affecting the heat transfer from the motherboard, causing an increase in the local air temperature. Furthermore, the PCMCIA cards and the power supply board obstruct the heat flow from the motherboard to the compartment walls. Therefore, not only do the PCMCIA cards and the power supply board heat the motherboard, but also they act as additional thermal resistors in the overall compartment thermal circuit. Thus, the increase in die temperature is believed to result from the increased compartment heat load, as well as thermal interaction between the motherboard and the other assemblies within the compartment.

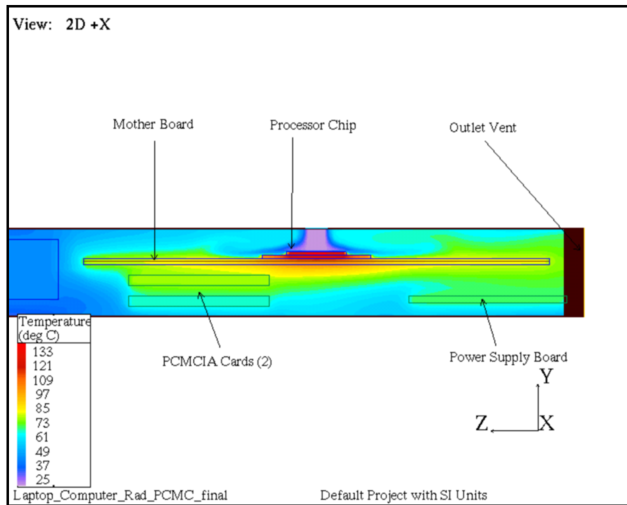

Figure 9 *- Side View Temperature Contour at Jet Centerline*

C. *Improved Design*

In an effort to reduce the die temperature an alternate design was considered. The configuration was modified such that the PCMCIA cards and the power supply were located above the motherboard in order to eliminate the heating of the motherboard by the PCMCIA cards and power supply board. The redesign involved shifting the motherboard 10mm down in the Y direction, and shifting the PCMCIA cards and the power supply board up 10mm in the Y direction. The location of PCMCIA cards and the power supply boards was such that they did not interfere with the impinging part of the flow. A temperature contour showing the results for the improved design is shown in ***Figure 10***. The average die temperature went from 131C to 129C and the average board temperature from 102C to 98C. The reduction in motherboard temperature was most significant in the region near the power supply board, where the board temperature decreased from 82C to 76C.

A comparison of ***Figures* 9** and ***10*** also show that there is less thermal interaction between the various assemblies in the improved design. Therefore, there are two advantages to relocating the power supply board and PCMICA cards. First, the new location reduces parasitic heating of the motherboard. Second, by locating the assemblies in the region of the compartment where there is significant air velocity, a substantial amount of heat from the PCMCIA cards, power supply board and the motherboard exits the compartment through the outlet vent, decreasing the thermal interaction between the various assemblies.

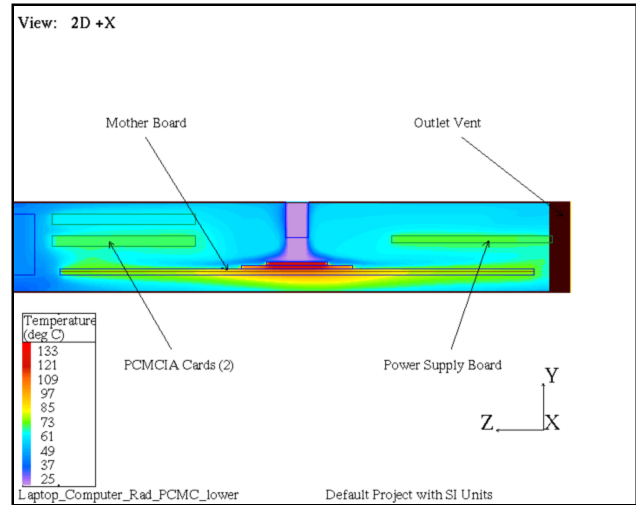

Figure 10 *– Temperature Contour at Jet Centerline Improved Design*

D. *Hybrid System*

Relocating the PCMCIA cards and the power supply board reduced the die temperature to about 129C. However, 129C is still in excess of the target temperature of 100C. To further reduce the processor chip operating temperature, an enhanced hybrid configuration was analyzed. The enhanced configuration was distinguished from the configuration of **IVC** by the presence of a miniature Copper-water heat pipe mounted on the underside of the motherboard. The purpose of the heat pipe was to provide a low resistance conduction path from the motherboard to the keyboard, with the keyboard serving as the condenser for the heat pipe. It was desired to utilize the large surface area of the keyboard to spread the heat, and provide a low resistance path for heat rejection by natural convection and radiation. ***Figure 11*** shows a view of the underside of the enhanced configuration with the heat pipe between the motherboard and the keyboard.

The heat pipe interfaces the motherboard with a 3.2mm thick Copper mounting block. The mounting block has the same in plane dimensions as the processor chip and mounts directly below it, on the underside of the motherboard. The overall length of the heat pipe is 104mm, and the cross section is 2mm x 8mm. The heat pipe was modeled as a solid conductive block with high thermal conductivity. The size and thermal characteristics are similar to the heat pipes described in [16] and [13]. In [16] the effective heat pipe thermal conductivity was specified as 4000W/mK, while a value of 10,000W/mK was used in [13]. The effective thermal conductivity used to model the heat pipe of this study was treated as a parameter. Cases were run with effective thermal conductivity values of 1000W/mK and 5000W/mK. A

thermally conductive adhesive was assumed at the following interfaces: mounting block/mother board, heat pipe/mounting block, heat pipe/keyboard. The thermal resistance due to the adhesive material was .5cm^{2}C/W [13].

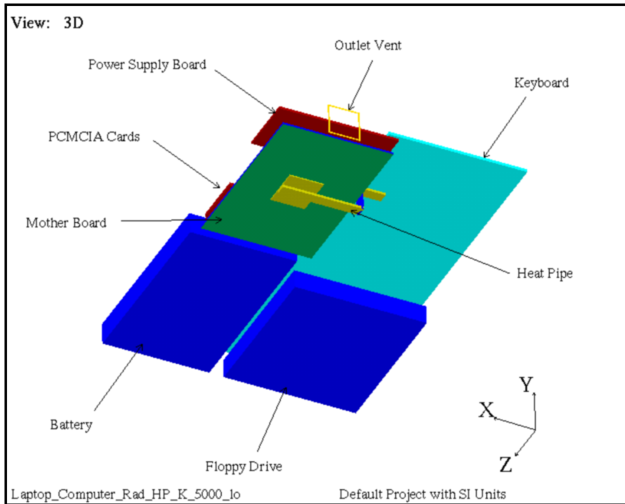

***Figure 11** – FLOTHERM™ Model of Enhance Laptop (view looking up from bottom)*

The combined heat pipe/JI configuration exploits the respective cooling strengths of the heat pipe and the impinging jet, with the goal creating a system superior to the separate configurations. Further, by splitting the heat between jet and the heat pipe, it was anticipated that the combined cooling scheme would be capable of cooling higher power systems than the respective separate configurations. The high heat transfer rates of the jet use extremely low mass flow rates that provide near passive cooling for the motherboard and processor chip. The heat transport capabilities of the heat pipe were used to efficiently transport heat from the motherboard to the keyboard, effectively reducing the motherboard heat load by the amount of heat that exits through the heat pipe. One of the weaknesses of heat pipes is that active cooling is often required at the heat pipe condenser. By using the large surface area of the keyboard to dissipate heat by natural convection and radiation, active cooling at the condenser is not required and the system is still near passive.

The addition of the heat pipe was found to dramatically improve the overall thermal performance of the entire compartment. ***Figure 12*** contains temperature contours for the improved configuration with and without heat pipes. Adding the heat pipe reduced the average board temperature was reduced from 98C to 85C and the average die temperature from 129Cto 111C. The temperature decrease is due to the large amount of heat (approximately 4W) that was transported from the motherboard to keyboard via the heat pipe. The heat pipe essentially reduces the motherboard heat load by the amount of heat that exits through the heat pipe itself. As one would expect, transferring heat from the motherboard to the keyboard with the heat pipe did increase the average keyboard temperature (from 37C to 50C). However, according to [4], keyboard temperatures up to 55C-60C are considered to be within the acceptable temperature range.

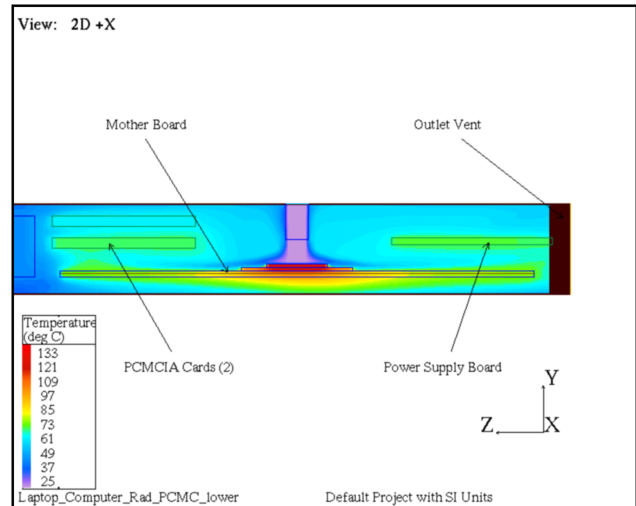

(a)

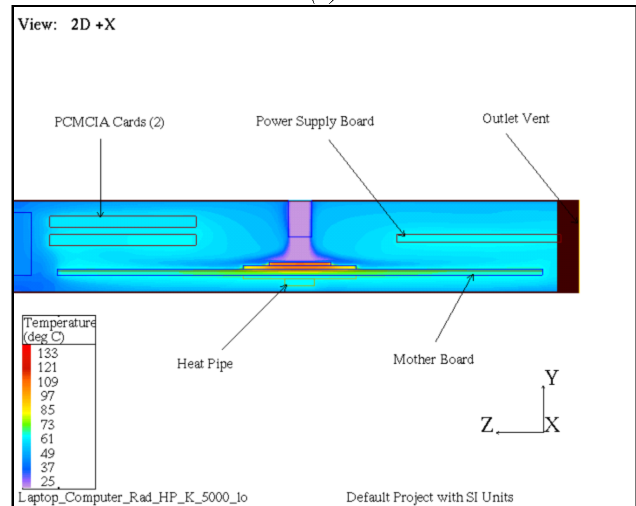

(b)

***Figure 12** – Side View Temperature Contours at Jet Centerline*

(a) Improved Design, (b) Improved Design with Heat Pipe

To gain an appreciation for the superior thermal performance of the hybrid laminar jet/heat pipe system, an additional configuration was analyzed that contained only the heat pipe (k=5000W/mK) and no jet. The heat pipe only, jet only and hybrid systems are compared in ***Table** 7*. The performance of the heat pipe only system was the worst, followed by jet only system, which was 24C cooler at the die. However, the die temperatures resulting from the heat pipe only and jet only systems are well above the allowable die temperature of 100C. By exploiting the strengths heat pipe and the jet, the combined system results in superior thermal performance and a die temperature that is much closer to the maximum allowable temperature.

Table 7 *- Temperature Results for Heat Pipe Only, Jet Only and Combined System*

Configuration	Avg. Die Temp. (C)	Avg. Board Temp.(C)
Heat Pipe Only	153	111
Jet Only	129	98
Combined Jet/Heat Pipe	111	85

The heat pipe results referred to until this point represent configurations where the heat pipe thermal conductivity was specified as 5000W/mK. To determine the sensitivity of the results to the specified heat pipe conductivity, an additional case was run with the conductivity set at 1000W/mK. The resulting die temperature increased by approximately 3C to 114C and the heat flow into the heat pipe decreased from 3.9W to 3.3W. Even though the heat pipe thermal conductivity was reduced by a factor of 5, the die temperature rise above ambient increased by only 3.5%. Thus, even if the heat pipe thermal conductivity was as low as 1000W/mK, the thermal resistance of the heat pipe is so low compared to the convection and radiation paths, a dramatic increase improvement in thermal performance was realized.

In a final effort to reduce die temperature, the model of the hybrid system was analyzed to see if there were features of the model that might be overly conservative, or not physically representative of an actual laptop computer other than the underlying steady state power dissipation assumption (see **V**). In the simulation results reported to this point there was not a conductive path between the motherboard and the laptop walls. In reality, there are conductive paths between the motherboard and compartment walls. In particular, the electrical connectors, brackets and hardware that are used throughout the compartment will help to spread, and dissipate heat. The inclusion of the mechanical details in the model adds unnecessary complication. Nonetheless, a simple test case was run to determine whether or not the lack of this conduction was giving overly conservative results. A conductive solid bar with a relatively high k (10 W/mK), with the same cross section as the motherboard, was added to fill the gap between the motherboard and compartment X high wall. The results revealed that adding the conduction path reduced the die temperature from 111C to 110.5C which, in turn, indicates that the model's lack of conduction path between the motherboard and die in the models is not significant.

E. Summary of Full Sized Configurations

The simulations of the full sized JI cooled laptop resulted in higher temperatures within the compartment, compared to the simplified configuration of **III**. The increase in operational temperatures is due mostly the increased compartment heat load and the resulting thermal interaction between the various assemblies. ***Table 8*** summarizes the results of the simulations. The baseline configuration resulted in a die temperature of 131C. By re locating the PCMCIA cards and the power supply board above the motherboard, the average die temperature was reduced to 129C, while the average motherboard temperature was reduced to 98C. A hybrid configuration, which included a Copper-water heat pipe mounted on the underside of the motherboard, provided the best thermal performance for the laptop configuration analyzed. While the hybrid cooling system did not cool the processor chip to below 100C, the results of the study indicate that JI cooling is in fact feasible for the cooling of the processor chips inside laptop computers. One of the key findings of the parametric studies of **III** was the sensitivity of the results to the applied heat load. While the hybrid-cooling plan did not quite satisfy the thermal requirements for the configuration analyzed, it could easily satisfy the thermal requirements for a similar system that has a slightly lower heat load and or a slightly different overall heat distribution.

Table 8*– Summary of Full Sized Laptop Simulations*

Configuration	Avg. Die Temp. (C)	Avg. Mother Board Temp. (C)	Heat Pipe Conductivy (W/mK)	Heat Pipe Heat Flow (W)
Baseline - Jet Only	131	102	-	-
Improved Design - Jet Only	129	98	-	-
Improved Design - Heat Pipe Only	153	111	5000	6.0
Improved Design - Heat Pipe and Jet	114	85	1000	3.3
Improved Design - Heat Pipe and Jet	111	88	5000	3.9

Another point regarding JI cooling that has not been addressed up until this point is the overall efficiency of the cooling solution. In [13] a similar laptop configuration was considered, though the configuration of the processor was different and processor heat load was slightly lower (8W vs. 10W). The thermal management plan used was a high volume flow rate cooling scheme, consisting of a $3ft^3$/min fan, Copper-water heat pipe, and a 25.4mm x 28mm x 12mm aluminum heat sink. In comparing the two systems the overall thermal performance was similar. However, it is important to note that the JI provides nearly the same level of cooling, while requiring only $.32ft^3$/min of air. The low volume flow required reduces system pressure drop and allows for the use of a smaller fan, which saves battery power. The required input power for a $3ft^3$/min 5VDC fan at a pressure drop of $.15inH_20$ is approximately .65W [17]. Conversely, a smaller 5VDC fan sized to meet the flow requirements of the JI configuration ($.32ft^3$/min at a pressure drop of $.03\ inH_20$) requires an input power of only .33W [18]. Thus, the JI configuration is more efficient as it provides comparable cooling while requiring about half of the input power. Furthermore, the high flow rate cooling scheme of [13] uses an aluminum heat sink, which is not required for the JI configuration. Thus, the JI configuration provides comparable cooling, but is simpler and more efficient than the high volume flow rate cooling scheme of [13].

V. CONCLUDING REMARKS

A detailed numerical study on the characterization of laminar jet impingement cooling in portable computer applications has been completed. The first part of the study was dedicated to studying the impinging jet in a simplified CPU compartment, while the second part of the

study demonstrated proof of concept by applying JI cooling to a configuration representative of a full sized laptop computer. The results of the study indicate the efficiency of JI heat transfer. The maximum chip heat load that can be cooled by a laminar jet (Re=1500, V=3.75m/s) is about 10W. Of the full sized models considered a combined JI/heat pipe system was resulted in the best thermal performance with a die temperature of 111C.

Finally, it should be noted that the underlying steady powering assumption for all components is not realistic. In most applications, power and heat economy measures are employed such that components are powered when needed and cooing fans are energized cyclically. Nevertheless, the neglect of this unsteady reality reinforces the positive conclusions of this study in die temperatures are probably overpredicted by several degrees.

ACKNOWLEDGEMENTS

An Aldo Miccioli Scholarship awarded to the first author by Raytheon Company made this research possible. Thanks are also extended to Flomerics Inc. for providing Tufts with FLOTHERM™ 2.2. A.J. Bettencourt, Scott Bittman and Vincent Miraglia for their assistance in conducting the experimental measurements.

VI. REFERENCES

1. T. Kobayashi, T. Ogushi, N. Sumi, and M. Fujii, "Thermal Design of an Ultra-Slim Notebook Computer", *IEEE Intersociety Conference on Thermal Phenomena*, 1998

2. J. Rujano, R. Cardenas, M. Rahman, W. Moreno, "Development of a Thermal Management Solution for a Ruggedized Pentium Based Notebook Computer", *IEEE Intersociety Conference on Thermal Phenomena*, 1998

3. J. Campbell, W. Black, A. Glezer, and J. Hartley, "Thermal Management of a Laptop Computers with Synthetic Air Micro-Jets", *IEEE Intersociety Conference on Thermal Phenomena,* 1998

4. H. Xie, M. Aghazadeh, W. Lui, and K. Haley, "Thermal Solutions to Pentium® Processors in TCP in Notebook and Sub-Notebooks", *IEEE Transactions on Components, Packaging, and Manufacturing Technology-Part A*, Vol. 19, No. 1, pp. 52-65, 1996

5. T. Nguyen, M. Mochizuki, K. Mashiko, Y. Saito, I. Sauciuc, and R. Boggs, "Advanced Cooling System Using Miniature Heat pipes in Mobile PC", *1998 IEEE Intersociety Conference on Thermal Phenomena*, pp. 507-511, 1998

6. S. Polat, B. Huang, A. Mujumdar, and W. Douglas, "Numerical Flow and Heat Transfer Under Impinging Jets: A Review", *Annual Review of Numerical Fluid Mechanics and Heat Transfer*, Vol. 2, pp. 157-197, 1989

7. J. Wheeler and S. Neti, "Heat Transfer from a Semi-Confined Impinging Laminar Jet", *National Heat Transfer Conference*, Aug., 1999

8. K. Ichimiya and N. Hosaka, "Experimental Study of Heat Transfer Characteristics due to Confined Impinging Two-Dimensional Jets", *Experimental Thermal and Fluid Science*, Vol. 5:803-807, 1992

9. Z. Lin, Y. Chou, Y. Hung, "Heat Transfer Behaviors of a Confined Slot Jet Impingement", *International Journal of Heat and Mass Transfer*, Vol. 40, No. 5, pp. 1095-1107, 1997

10. J.R. Guarino, V.P. Manno, "Laminar Jet Impingement Convective Heat Transfer in Partially Vented Enclosures Typical of Portable Computer Applications", *First MIT Conference on Computational Fluid and Solid Mechanics*, 2001

11. J.R. Guarino, "Enhanced Cooling of Portable Computers Using Mixed Natural and Laminar Air Jet Impingement Convection, Masters Degree Thesis, Tufts University, 2000

12. Intel® Corporation, 2000 Packaging Data Book

13. Flomerics Inc., FLOTHERM™, Tutorial: Thermal Modeling of Laptop Computers

14. Flomerics Inc., FLOTHERM™ 2.2 Users Guide

15. A.F. Mills, Heat and Mass Transfer, Richard Irwin Inc, 1995

16. R. Viswanath, I. Ali, "Thermal Modeling of High Performance Packages in Portable Computers", *IEEE Transactions on Components, Packaging, and Manufacturing Technology-Part A*, Vol.20, No.2, pp. 230-240, 1997

17. Product data sheet for Sunon Co. Ultra Thin DC Fan, P/N,KD0503PEB1-8, www.sunon.com

18. Product data sheet for Indek Co. DC Fan, P/N HDF2510L-12MB, www.indek.com